

Finite-element Simulations of a Volumetric Scanning Microwave Probe for Imaging at the Nanoscale

A. O. Oladipo^{1,2}, M. Kasper³, S. Lavdas², G. Gramse³, F. Kienberger⁴, N. C. Panoiu²

¹Bio-Nano Consulting, 338 Euston Road, London NW1 3BT, United Kingdom

²University College London, Electronic and Electrical Engineering Department, Torrington Place, London WC1E 7JE, United Kingdom

³Johannes Kepler University Linz, Gruberstrasse 40, 4020 Linz, Austria

⁴Agilent Technologies Austria GmbH, Gruberstrasse 40, 4020 Linz, Austria
Abiola.Oladipo@bio-nano-consulting.com

Abstract – Many electrical scanning probe microscopy (SPM) techniques suffer from parasitic stray EM field contributions, which give rise to low signal to noise ratio and make the image retrieval process more difficult. Here, we validate via computational modeling a calibration procedure that employs three calibration standards and three complex coefficients to obtain a black-box transfer function between the systemic reflection coefficient and the reflection coefficient at the tip of the probe, from which the impedance, capacitance and dielectric constant of nano-sized structures can be determined. We find that a 1° variation in the inclination angle of the cantilever can cause a 10% variation in the bulk systemic impedance. Experimental scanning microwave microscope measurements agree with our simulation results.

I. INTRODUCTION

A detailed understanding of the physical properties and interactions of materials at very small length scales has become of great interest in many areas of research and industries such as solid-state physics [1], material science [2] and biological sciences [3]. Several microscopy techniques have been used to characterize the physical properties of materials at different length-scales. For example, optical and electron microscopes as well as atomic forces microscopes have been used to obtain detailed structural and tomographic images of samples[4]. Furthermore, SPM techniques such as scanning capacitance microscopy [5], electrostatic force microscopy [6], scanning impedance microscopy [7] and scanning polarization force microscopy [8] have been shown to give the local dielectric properties of materials at the nanoscale. Among several limitations of these aforementioned technologies (effects of probe geometry, inherent weak polarization signals, poor stability and sensitivity in detection systems), the presence of non-local (stray) field contributions complicates the quantitative analysis of tip sample interactions and make the calibration of the microscopy system difficult [6].

In this work, we performed the finite element analysis of the electromagnetic interactions between the platinum probe of a scanning microwave microscope (SMM) and several bulk calibration samples. In SMM, a vector network analyzer (VNA) is combined with an atomic force microscope and sends a continuous microwave signal (1-20 GHz) to the conductive tip. Depending on the electric sample properties and the impedance of the tip-sample interface, part of the microwave signal is reflected and measured by the PNA as the scattering S11 reflection signal. We find good agreement between our computational and experimental results from a calibration experiment. Our results validate the calibration algorithm described in [9] where three electrically different calibration standards and three complex correction coefficients were used. In order to extend the application of the aforementioned calibration algorithm to arbitrary sample, it is important to understand how the changes in the EM field configuration during sample exchange affect the measured parameters (impedance). Here, we show the effect of varying the inclination angle of the cantilever and cone on the impedance of the SPM system.

II. THE CALIBRATION SAMPLE AND ALGORITHM

The calibration sample, presented schematically and topographically in Fig. 1B and Fig. 1C, respectively, comprises of a relatively thick (500 μm) layer of doped silicon substrate on top of which a staircase layer (200 nm) of silicon oxide SiO_2 was deposited. Each step in the SiO_2 layer was 50 nm thick. On each step of the SiO_2

layer, various diameters (1 μm , 2 μm , 6 μm and 10 μm) of gold nano-pads (300 nm height) were deposited. In the calibration algorithm discussed in [9], three gold nano-pads of varying electrical properties were selected and used to generate the three complex coefficients e_{00} , e_{01} , and e_{11} required for a black-box transfer function [as introduced in Eq. (1)] that relates the bulk system (shown in Fig 1A) $S_{11,m}$ and the $S_{11,probe}$ at the tip. The complex impedance Z_{probe} at the tip was calculated from the reflection coefficient $S_{11,probe}$ by using Eq. (2).

$$S_{11,probe} = \frac{S_{11,m} - e_{00}}{e_{01} + e_{11}(S_{11,m} - e_{00})} \quad (1) \quad Z_{probe} = Z_{ref} \frac{1 + S_{11}}{1 - S_{11}} \quad (2)$$

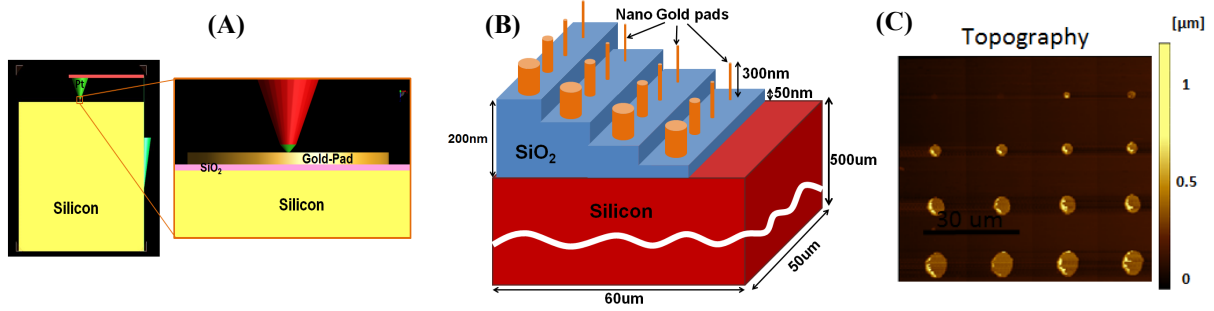


Fig. 1: (A) An image of the full system model setup in EMPro. (B) Schematic diagram and (C) topographic image of the sample used in the experimental measurements.

III. FINITE ELEMENT ANALYSIS OF THE CALIBRATION SAMPLE

In order to validate the calibration algorithm presented in [9], we performed a finite element analysis of the electromagnetic interactions at the tip using Agilent's EMPro. In Fig 2A, we show the low sensitivity (due to stray fields) of the non-calibrated system capacitance to variations in the gold nano-pad diameter. In order to model a calibrated SMM system in contact mode, only the small ($r = 100$ nm) nano-sphere at the very end of the metallic tip was considered in order to avoid the stray field contributions from the probe and the cantilever. The model geometry (inset of Fig. 2B) used in our simulations based on the finite element method (FEM) considered the case when the SiO_2 layer is 100 nm thick and the gold nano-pad diameters of 1 μm , 2 μm , 6 μm and 10 μm . The entire computational structure was enclosed in a large air-box with perfectly matched layer as the boundary condition. As excitation we used an AC voltage of 1 V, applied to the nano-sphere relative to the ground, at the bottom plane of the entire simulation domain. We present in Fig. 2B a plot of the tip capacitance [$C_{probe} = 1/(2\pi\nu X_c)$] against the diameter of the gold nano-pads. In this analysis X_c is the capacitive reactance at the metallic probe. A good agreement can be seen between our modeling results and the experimental data obtained from the calibration algorithm. This result validates the three standards calibration algorithm introduced and discussed in [9].

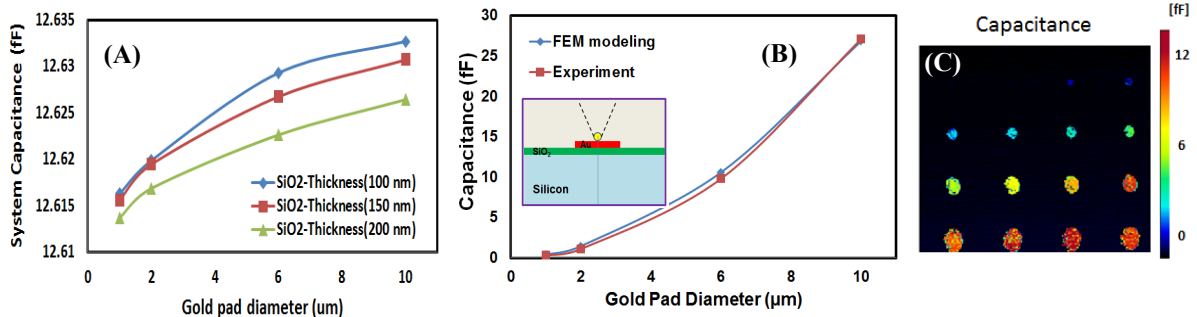


Fig. 2: (A) Plot of system capacitance with stray fields contribution. (B) The capacitance of the metallic tip only, calculated for various gold nano-pad diameter. (C) The capacitance image of the sample, derived from experimental measurements. A good agreement was found between the FEM modeling and the experimental results.

In order to extend this calibration algorithm to the characterization of arbitrary samples, the effect of variations in the structure of the SMM system (illustrated schematically in Fig. 3A) during sample exchange needs to be investigated. In this section, we outline the main conclusions of this study by presenting in Fig. 3B the effect of varying the main system parameter, namely, the inclination of the cantilever and cone, on the calculated bulk systemic impedance. Our numerical simulations show that a 1° increase in the inclination angle θ , can cause about 10% increase in the total systemic impedance. This finding suggests that changes in the SMM system could have a significant impact on the measurement sensitivity after calibration.

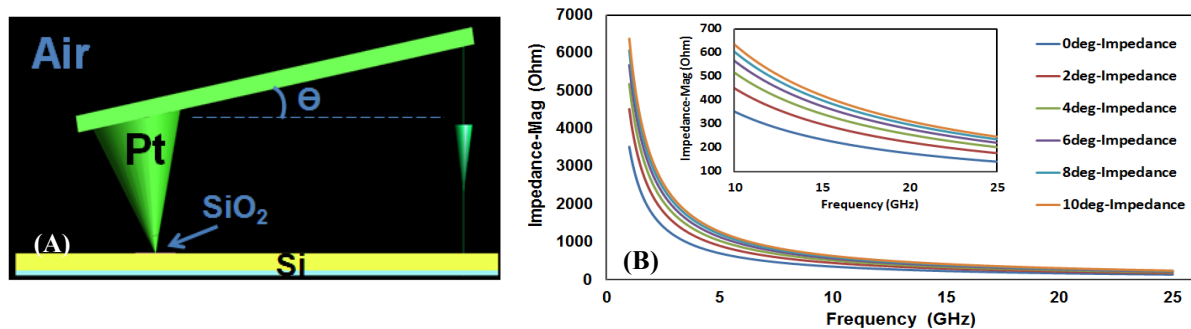


Fig. 3: (A) Schematics of the system investigated. (B) Plot of impedance vs. frequency calculated for various inclination angle of the probe.

IV. CONCLUSION

We have performed a theoretical analysis and numerical validation of an experimental three standard calibration algorithm for 3D imaging at the nanoscale. We found good agreement between our computational results and the experimental data. We also investigated the dependence of the bulk systemic impedance on several system parameters, the main conclusion being that variations in the SMM system including tip and substrate require a new calibration of the system so that correct results are still obtained.

ACKNOWLEDGEMENT

This work has been supported by the EU-FP7 (NMP-2011-280516, “VSMMART-Nano” and PEOPLE-2012-ITN-317116, “NANOMICROWAVE”). The authors would like to thank C. Rankl and M. Moertelmaier from Agilent Austria for helpful technical discussions.

REFERENCES

- [1] A. Tselev *et al.*, “Near-field microwave scanning probe imaging of conductivity,” *Nanotechnology*, vol. 23, 385706, 2012.
- [2] S. Gomez-Monivas *et al.*, “Quantitative theory for the imaging of conducting objects in electrostatic force microscopy,” *Appl. Phys. Lett.*, vol. 89, 173122, 2006.
- [3] E. Mikamo-Satoh *et al.*, “Electrostatic force microscopy: imaging DNA and protein polarizations one by one,” *Nanotechnology*, vol. 20, 145102, 2009.
- [4] K. M. Lang *et al.*, “Conducting atomic force microscopy for nanoscale tunnel barrier characterization,” *Rev. Sci. Instrum.*, vol. 75, 2726, 2004.
- [5] D. T. Lee, J. P. Pelz, and B. Bhushan, “Scanning capacitance microscopy for thin film measurements,” *Nanotechnology*, vol. 17, pp. 1484-1491, 2006.
- [6] L. Fumagalli *et al.*, “Label-free identification of single dielectric nanoparticles and viruses with ultraweak polarization forces,” *Nature Mater.*, vol. 8, 3369, 2012.
- [7] K. Kathan-Galipeau *et al.*, “Direct probe of molecular polarization in de novo protein electrode interfaces,” *ACS Nano*, vol. 5, pp. 4835-4842, 2011.
- [8] J. Hu, X. Xiao, and M. Salmeron, “Scanning polarization force microscopy: A technique for imaging liquids and weakly adsorbed layers,” *Appl. Phys. Lett.*, vol. 67, pp. 476-478, 1995.
- [9] H. P. Huber *et al.*, “Calibrated nanoscale capacitance measurements using a scanning microwave microscope,” *Rev. Sci. Instrum.*, vol. 81, pp. 9, Nov 2010.